CALCULATION OF THE KICK MAPS GENERATED BY A HOLLOW ELECTRON LENS FOR STUDIES OF HIGH-ENERGY HADRON BEAM COLLIMATION*

G. Stancari[†], M. Chung, A. Valishev, Fermilab, Batavia, IL 60510, USA
V. Moens, EPFL, Lausanne, Switzerland, H. J. Lee, Pusan National University, Korea

Abstract

Collimation with hollow electron beams is a technique for halo removal in high-power hadron beams. It was experimentally studied at the Fermilab Tevatron collider using electron lenses and it is being considered as an option to complement the collimation system for the LHC upgrades. In the ideal case, the magnetically confined electron beam has a hollow, axially symmetric current-density distribution, whose fields affect the beam halo, leaving the core of the circulating beam unperturbed. We address the effects of imperfections in the current density based upon profiles measured in the Fermilab electron lens test stand. We also study the effect of the bends used to inject and to extract the electron beam from the overlap region. The calculated field distributions will serve as inputs for tracking simulations, which are needed to estimate the effects of the electron lens imperfections on beam core dynamics, such as nonlinearities and emittance growth.

INTRODUCTION

Hollow electron beam collimation is a new technique for collimation and halo scraping of intense hadron beams in storage rings and colliders [1]. In a hollow electron beam collimator, a magnetically confined, pulsed, low-energy electron beam with a hollow current-density profile overlaps with the circulating beam over a short section of the ring. Figure 1 shows the layout of one of the Tevatron electron lenses. The beam is formed in the electron gun inside a conventional solenoid and guided by strong axial magnetic fields. Inside the superconducting main solenoid, the circulating beam interacts with the electromagnetic fields generated by the charge distribution of electrons. The electron beam is then extracted and deposited in the collector. The halo of the circulating beam can be smoothly scraped. The core is unaffected if the distribution of the electron charge is axially symmetric. One cause of asymmetry is the space-charge evolution of the electron beam as it propagates through the electron lens. Another source of asymmetry are the bends that are usually used to inject and extract the electron beam from the interaction region. Although small, these asymmetries may have detectable effects on

core lifetimes and emittances because of their nonlinear nature, especially when the current of the electron pulse is changed turn by turn to enhance the halo removal effect by resonant excitation of selected particles.

In this paper, we discuss the effects of these asymmetries from experimental data and from calculations. In particular, the asymmetries in the charge distribution are translated into transverse kick maps for the circulating beam. These kick maps are provided as inputs for numerical tracking simulations of the Fermilab Tevatron collider and of the Large Hadron Collider at CERN with the Lifetrac or Six-Track codes. This work is in support of a conceptual design for a proposed hollow electron beam collimator for the LHC upgrade [2]. The same techniques can be applied to different current-density profiles (Gaussian, flat, etc.) to study perturbations in nonlinear integrable optics with electron lenses for the IOTA ring at the Fermilab ASTA facility [3].

AZIMUTHAL ASYMMETRIES

Two-dimensional azimuthal asymmetries of the electron current density in the overlap region inside the main solenoid (neglecting the injection and extraction regions) may be caused by the space-charge evolution of the hollow electron beam as it propagates through the electron lens (diocotron instability), or by imperfections in the electron gun geometry, magnetic field lines, etc.

Electron guns are characterized at the Fermilab electron-lens test stand. Current-density profiles are measured as a function of beam current and axial magnetic field. Space-charge evolution of the electron beam profiles is mitigated by increasing the guiding magnetic fields. The measured profiles are used to calculate the corresponding transverse electric fields inside the beam pipe using the Poisson
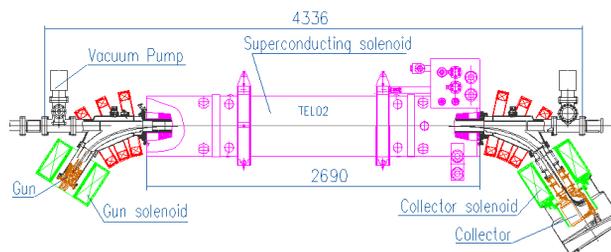

Figure 1: Layout of a Tevatron electron lens. (Dimensions in millimeters.)

solvers of the Warp plasma particle-in-cell code [4]. A few examples of these calculations can be found in Ref. [5]. Inside the hole of the electron beam, where no charge is present, the potential satisfies Laplace's equation and the effect of the asymmetries can be characterized as a superposition of multipoles. Elsewhere, a more general parameterization is necessary. This approach was used to compare calculated and measured halo removal rates in the Tevatron [6]. For the Tevatron lattice and tune working point, the only azimuthal asymmetry seen to cause extra losses in the core was the quadrupole component in a particular resonant mode (pulsing the electron beam every 6th turn). Calculations for the LHC are under way and will be presented in the conceptual design report.

EFFECT OF BENDS

In an electron lens, toroidal bends are used for injecting and extracting the electron beam (Figure 1). To study whether the curved charge distribution of electrons has a significant effect on the dynamics of the circulating beam, we rely on the Tevatron experiments and on calculated kick maps.

Most of the Tevatron experiments on hollow electron beam collimation were done in continuous mode: the electron current was kept constant turn by turn. Under these conditions, no deteriorations of core lifetimes or luminosities were observed. For the LHC, to extend the range of achievable halo removal rates, resonant operation is also being considered: in this mode, the voltage in the electron gun is changed turn by turn according to a sinusoidal function, in resonance with betatron oscillations, or with the same amplitude, skipping a given number of turns [7]. Resonant operation was used for abort-gap cleaning in the Tevatron [8], but no systematic experimental studies were done on the effects of time-varying pulse amplitudes on the beam core. For this reason, numerical tracking studies are planned, and here we describe the calculation of the kick maps to be used as inputs.

The parameters of the proton beam are used to calculate beam sizes in the interaction region. We assume a round proton beam with a typical rms beam size $\sigma_p = 0.317$ mm. The hollow electron beam is represented by a cylindrical bent pipe with a curvature radius $R = 0.7$ m, inner radius $r_i = 1.27$ mm $= 4\sigma_p$, and outer radius $r_o = 2.39$ mm $= 7.5\sigma_p$. The ratio between the outer and the inner radius is chosen to reproduce the dimensions of the cathode in the existing 1-inch hollow electron gun [5, 9]: $(12.7$ mm$)/(6.75$ mm$)$. The bent tube of electrons spans a bend angle of $\theta = 30$ deg. A total of $N_e = 1048576 = 2^{20}$ electron macroparticles is used to reproduce the static charge density distribution of a 1-A, 5-keV electron beam. The z-axis is chosen along the direction of the circulating proton beam. The x-axis points horizontally outward. The upward direction is represented by the y-axis. The origin of the coordinate system coincides with the point where the axis of the bent electron beam intersects the axis of the circulating beam (Figure 2).

A multigrid Poisson solver within the Warp particle-in-cell code is used to calculate the electrostatic fields. The boundary conditions are defined by a long cylindrical main beam pipe and by a cylindrical injection beam pipe stub, joining the main pipe at an angle (Figure 2). This arrangement is a simplified version of the injection scheme in the Tevatron electron lenses (Figure 1). Both pipes have an inner radius $r_{\text{pipe}} = 40$ mm.

Space is subdivided into 2 discrete grids, a coarse one (2-mm spacing) covering the whole space, and a fine one (0.1 mm) around the central trajectory of protons. The transverse coverage of the fine mesh, $-10\sigma_p \le x, y \le 10\sigma_p$, is designed to obtain kick maps for both the core and the halo of the proton beam.

Figure 2 shows the electrostatic potential $V(x, y, z)$ on the xz-plane of the bend. The electrostatic fields E_x and E_y are integrated over straight paths to calculate the transverse momentum kicks $\Delta p_{x,y}$ experienced by the circulating proton beam:

$$k_{x,y}(x,y) \equiv \int_{z_1}^{z_2} E_{x,y}(x,y,z)\,dz, \qquad (1)$$

$$\Delta p_{x,y} = \int_{t_1}^{t_2} F_{x,y}\,dt = \frac{q}{v_z}\int_{z_1}^{z_2} E_{x,y}\,dz = \frac{q}{v_z}k_{x,y}, \qquad (2)$$

where q, v, and p are the charge, velocity, and momentum of the circulating beam, F is the electrostatic force, t is time, and the integrated fields k_x and k_y are later loosely referred to as 'kicks.' Only transverse kicks are considered, as the longitudinal kicks of two symmetric bends cancel out. The transverse kicks due to two bends, on the other hand, have the same sign and will add up. The typical angles of the proton trajectories are of the order of $\sigma_p' = 1.6\ \mu$rad, so the resulting position variations over the length of the bend can be neglected. For 7-TeV protons, an integrated field of 10 kV generates an angular deviation of 1.4 nrad. The kick maps on the fine mesh are represented as contour plots in Figure 3. Protons on axis experience a negative horizontal integrated field of -9.1 kV, whereas
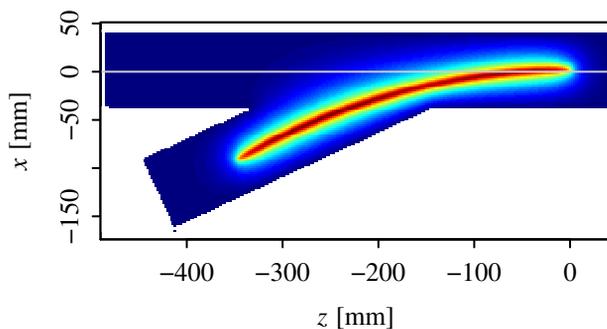
Figure 2: Conductor geometry and calculated electrostatic potential on the plane of the bent electron distribution. Dark red corresponds to -1.2 kV, dark blue represents 0 V. The horizontal gray line is the axis of the proton beam.

the vertical kick vanishes. The vertical kick on the plane of the bend is zero.

For tracking simulations, one can interpolate the given kick maps in 2 dimensions for each particle. Alternatively, to speed up calculations, one can use an analytical formulation of the functions $k_x(x,y)$ and $k_y(x,y)$. We use a parameterization in terms of the outer product of 1-dimensional Chebyshev polynomials in x and y up to a given order N. Because of the symmetry of the charge distribution, the horizontal kicks are even functions of y and only contain even powers of the vertical coordinate, whereas the vertical

kicks are odd functions of y. At order $N = 7$, for instance, the standard deviation of the residuals of this interpolating model is about 150 V.

To study the sensitivity of the results to the geometry of the system, cases with different beam pipe radii and injection angles are simulated. The chosen beam pipe radii were 35 mm, 40 mm (reference case), and 45 mm. The chosen bend angles were 25 deg, 30 deg (reference case), and 35 deg. The changes in geometry considered in this study amount to a change in the kicks of less than 300 V.

Further details on the calculation of these kick maps can be found in Ref. [10].

CONCLUSIONS

We studied some of the effects of electron-lens asymmetries on the circulating beam for hollow electron beam scraping. Two-dimensional current-density distributions are measured in the Fermilab electron-lens test stand and are used to calculate the transverse electric field distributions for tracking simulations. The electrostatic fields generated by the injection and extraction bends in an electron lens were also estimated. A bent, 1-A, 5-keV electron beam creates nonlinear transverse integrated electric fields of the order of 10 kV. Kick maps are provided on a fine grid for 2-dimensional interpolation and as coefficients of truncated power series of orthogonal polynomials for evaluation with analytical formulas in numerical tracking codes.

REFERENCES

[1] G. Stancari et al., Phys. Rev. Lett. **107**, 084802 (2011).

[2] G. Stancari et al., in these Proceedings, FERMILAB-CONF-13-355-APC.

[3] S. Nagaitsev et al., in Proceedings of the 2012 International Particle Accelerator Conference (IPAC12), New Orleans, LA, USA, May 2012, p. 16, FERMILAB-CONF-12-247-AD; A. Valishev et al., ibid., p. 1371, FERMILAB-CONF-12-209-AD-APC.

[4] J.-L. Vay, D. P. Grote, R. H. Cohen, and A. Friedman, Comput. Sci. Disc. **5**, 014019 (2012).

[5] V. Moens, Masters Thesis, École Polytechnique Fédérale de Lausanne (EPFL), Switzerland, FERMILAB-MASTERS-2013-02 and CERN-THESIS-2013-126 (August 2013).

[6] I. Morozov et al., in Proceedings of the 2012 International Particle Accelerator Conference (IPAC12), New Orleans, LA, USA, May 2012, p. 94, FERMILAB-CONF-12-126-APC.

[7] V. Previtali et al., in Proceedings of the 2013 International Particle Accelerator Conference (IPAC13), Shanghai, China, May 2013, p. 993, FERMILAB-CONF-13-154-APC; FERMILAB-TM-2560-APC (July 2013).

[8] X. Zhang et al., Phys. Rev. ST Accel. Beams **11**, 051002 (2008).

[9] S. Li and G. Stancari, FERMILAB-TM-2542-APC (August 2012).

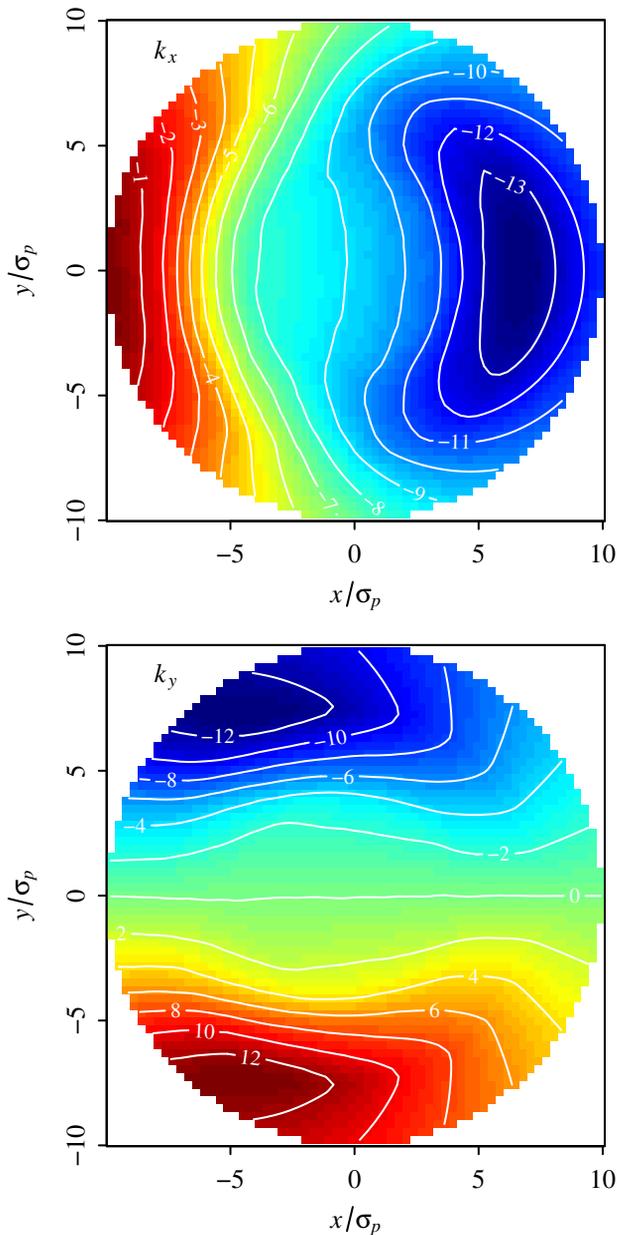[10] G. Stancari, FERMILAB-FN-0972-APC (September 2013).

Figure 3: Contour plots of the integrated fields k_x (top) and k_y (bottom) as a function of scaled transverse coordinate. The contour lines are labeled with the value of the integrated field in kilovolts.